processes

MDPI

Article

Potential Improvement in PM-NO_X Trade-Off in a Compression Ignition Engine by *n*-Octanol Addition and Injection Pressure

Qiwei Wang [1,2,*], Rong Huang [2,*], Jimin Ni [2] and Qinqing Chen [2]

[1] Postdoctoral Station of Mechanical Engineering, School of Automotive Studies, Tongji University, Shanghai 201804, China
[2] School of Automotive Studies, Tongji University, Shanghai 201804, China; njmwjyx@hotmail.com (J.N.); Chenqinqing@163.com (Q.C.)
* Correspondence: wangqiwei1987@hotmail.com (Q.W.); hr1209@tongji.edu.cn (R.H.); Tel./Fax: +86-021-69589980 (R.H.)

Abstract: *n*-Octanol, as an oxygenated fuel, is considered as one of the most promising alternative fuels, owing to advantages such as its low hygroscopic nature, high cetane number, and high energy content. However, the introduction of *n*-octanol leads to a higher viscosity and latent heat of evaporation (LHOE), affecting the combustion and emission performances of compression ignition (CI) engines. This study sheds light on the effect of injection pressures (IPs, ranging from 60 to 160 MPa) on the combustion and emission performances of a turbocharged CI engine, in conjunction with *n*-octanol/diesel blends. According to the proportion of oxygen content, the test fuels contain pure diesel (N0), N2.5 (2.5% oxygen content in the blending fuels), and N5 (5% oxygen content in the blending fuels). The results indicate that the blending fuels have little influence on the in-cylinder pressure, ignition delay (ID), and CA50, but they improve the brake thermal efficiency (BTE). In terms of emissions, with the use of blending fuels, the levels of carbon monoxide (CO), soot, and nitrogen oxides (NO_X) decrease, whereas emissions of hydrocarbons (HC) slightly increase. With increasing IP, the ID, brake specific fuel consumption (BSFC), HC, CO, and soot decrease significantly, and the BTE and NO_X increase. In addition, the combination of *n*-octanol and IP improves the trade-off between NO_X and soot and reduces the CO emissions.

Keywords: diesel engine; *n*-octanol/diesel; injection pressure; combustion; emissions

check for updates

Citation: Wang, Q.; Huang, R.; Ni, J.; Chen, Q. Potential Improvement in PM-NO_X Trade-Off in a Compression Ignition Engine by *n*-Octanol Addition and Injection Pressure. *Processes* **2021**, *9*, 310. https://doi.org/10.3390/pr9020310

Academic Editor: Jianbing Gao
Received: 18 January 2021
Accepted: 4 February 2021
Published: 7 February 2021

Publisher's Note: MDPI stays neutral with regard to jurisdictional claims in published maps and institutional affiliations.

Copyright: © 2021 by the authors. Licensee MDPI, Basel, Switzerland. This article is an open access article distributed under the terms and conditions of the Creative Commons Attribution (CC BY) license (https://creativecommons.org/licenses/by/4.0/).

1. Introduction

According to the World Energy Council, the demand for transport energy has a strong preference for heavier fuels such as diesel and jet fuels; it is expected that the consumption of heavier fuels will rise from 1.5 to 3.8 EJ by 2040 [1]. Moreover, it has also been reported that fossil fuels account for nearly 80% of the usage of primary energy; 58% of this primary energy is consumed by transportation [2]. The combustion of compression ignition (CI) engines results in high amounts of emissions such as CO_2 and toxic pollutants (soot and nitrogen oxides (NO_X)), which are likely to result in cardiovascular and lung cancer deaths once inhaled into respiratory tracts [3]. Therefore, there is an urgent need to find alternative clean energies to replace the use of oil. Recently, experimental investigations on oxygenated fuels have shown significant effects on emissions reduction [4,5]. Oxygenated fuels can restrain soot formation by oxidizing unsaturated hydrocarbons (HC), and suppressing the formation of soot among C atoms [6]. Thus, it has been generally recognized that oxygenated fuels can play considerable roles in overcoming the main challenges with respect to CI engines and in realizing technological breakthroughs and practical applications [7,8].

Alcohols, as a type of oxygenated fuel, have drawn significant attention in regards to combustion and emissions in CI engines, owing to their high oxygen content. Researchers have investigated low-carbon alcohols such as methanol and ethanol in the past decade [9]. However, their characteristics (such as their miscibility) limit their usability in CI engines,

owing to the stratification between different fuels [10]. In this regard, high-carbon chain alcohols offer excellent compatibility with diesel engines, owing to their low hygroscopic nature [11]. *n*-Octanol, with a higher cetane number (CN), heating value, and energy content, is more similar to diesel as compared with low alcohols [7,12,13]. Its higher flash point, lower vapor pressure, and less corrosive nature offer increased safety when used with diesel fuels [14]. Additionally, its relatively lower CN in contrast to that of diesel enhances the premixed combustion stage and improves the diffusion combustion stage, thereby decreasing soot emissions [15,16]. In terms of production, *n*-octanol can be obtained from non-food biomasses such as lignocellulosic biomasses; moreover, the emergence of bio-synthesis technology has greatly improved its feasibility for use in CI engines [17]. Considering all of the above advantages, the use of *n*-octanol as an alternative candidate to diesel has attracted significant attention from researchers.

Studies on the application of *n*-octanol have considered several perspectives. For example, Heuser et al. [18] conducted an experiment on a single-cylinder diesel engine powered by pure *n*-octanol; the particulate matter (PM) was reduced by approximately 20% compared to that of diesel, with little impact on the brake thermal efficiency (BTE) and NO_X emissions [19]. Deep et al. [20] evaluated different proportions of *n*-octanol-diesel blends (10–40% by volume) on combustion and emissions in CI engines. They found that carbon monoxide (CO) emissions decreased with an increase in *n*-octanol, whereas the HC emissions increased sharply. McCormick et al. [21] studied *n*-octanol/diesel blends at 2 wt% oxygen and found that the PM and NO_X emissions decreased by 12% and 3%, respectively. A combination of conventional B5 palm oil with added *n*-octanol and diethyl succinate was verified to enhance combustion quality and lower pollutants, as demonstrated by Phoon et al. [22]. Zhang et al. [23] investigated alcohol-diesel blends at four operating points from the European Stationary Cycle. A similar performance was found, and they concluded that longer-chain alcohols present substantial potential as compositions of mixed diesel fuels.

For a more comprehensive understanding of the utilization of *n*-octanol in CI engines, more detailed information is required regarding its combustion behaviors and emissions. A detailed chemical kinetic model on the oxidation process of *n*-octanol was built in a shock tube and jet-stirred reactor by Cai et al. [24]. They found that the ignition delay (ID) was sensitive to the H-abstraction reaction from the hydroxyl radicals and peroxy radical isomers. Overall, the hydroxyl functional group played the primary role in soot reduction. Bharti et al. [25] conducted a reactive molecular dynamics emulation on *n*-octanol under a range of equivalence ratios (0.5–2.0) at 2000–4000 K, aiming to understand the combustion characteristics. They concluded that the oxidation process of *n*-octanol was mainly initiated in two ways: a hydrogen absorption reaction from oxygen molecules, and the fracture of C-C bond. They proposed the reaction mechanisms for the main intermediate products and final products, which were related to build-ups of hydroperoxyl and hydroxyl radicals. Kerschgens et al. [26] further investigated the ignition behaviors, combustion, and pollutant formation from three different C8 fuels (di-n-buthylether, *n*-octane, and *n*-octanol) using kinetic mechanisms and an interactive flamelet approach. The results show that low soot emissions were achieved, the HC and CO emissions were mainly caused by different ignitability values (as reflected by the different CN), and the ID was partially influenced. To summarize, *n*-octanol/diesel blends exhibited fuel properties similar to those of diesel; more importantly, the emissions were reduced significantly. Therefore, *n*-octanol/diesel mixtures are expected to be the most promising alternatives to CI engines.

The injection pressure (IP) is one parameter among the numerous factors affecting the atomization process and fuel–air mixing, resulting in changed engine performance. Agarwal et al. [27] concluded that the number of larger-sized particles, CO_2, and HC in the exhaust emissions decreased substantially, and that they gained higher BTE and IP than under a single-cylinder diesel engine case. Zhang et al. [28] researched the influence of fuel spray characteristics and emissions on a heavy-duty CI engine. The results showed that the spray droplet diameter reduced with an increase in IP, leading to better fuel–air mixing,

thereby decreasing smoke and CO emissions. However, Celıkten et al. [29] concluded that the ID will be too short if the IP is too high; in such a case, the homogeneous mixed period decreases, resulting in poor combustion efficiency [30]. Gumus et al. [31] studied the impact of biodiesel–diesel blends and IP on a CI engine and concluded that almost all emissions, BTE, and brake specific fuel consumption (BSFC) gained optimally at 24 MPa fueled with B100. Puhan et al. [32] concluded that a *Calophyllum inophyllum* methyl ester injected with 22 MPa presented better performance and emission characteristics than other IPs in an experiment with a direct injection diesel engine. Hence, it is worth investigating the optimal values of the IP and *n*-octanol/diesel blends on the combustion and emission performances of a CI engine.

In summary, the impact from the IP as combined with *n*-octanol on a diesel engine has not been examined in the literature. To fill this gap, experiments were conducted in the present research to comprehensively study the combustion and emission behaviors of IPs in a turbocharged, four-cylinder CI engine, as powered by alternative *n*-octanol/diesel blend fuels.

2. Experimental Facility and Steps

2.1. Experimental Setup and Methods

All of the tests were performed on a four-cylinder, turbocharged, four-stroke diesel engine. The specifications are shown in Table 1. A more detailed schematic layout is depicted in Figure 1. In this study, a stable rotating speed of the engine was obtained by controlling a PowerLink eddy-current dynamometer, which maintained the speed in the range of 1500 $\pm$ 5 rpm. The engine experimental points of the test fuels corresponded to a brake mean effective pressure (BMEP) of 0.8 MPa. The injection timing was controlled at -4 crank angle degrees after top dead center, and the IPs used in this experiment were 60, 80, 100, 120, 140, and 160 MPa. The engine experimental conditions are listed in Table 2. The IP was accurately controlled with the INCA software. A Kistler 6061B pressure transducer was used to measure the in-cylinder pressure (ICP) signals from each cycle, transmit the signals to a charge amplifier, and record the results according to a Dewetron combustion analyzer. In addition, the in-cylinder temperature was calculated by combustion analyzer. The error rate of the pressure sensor was 0.01 MPa, and an average of 200 cycles was collected.

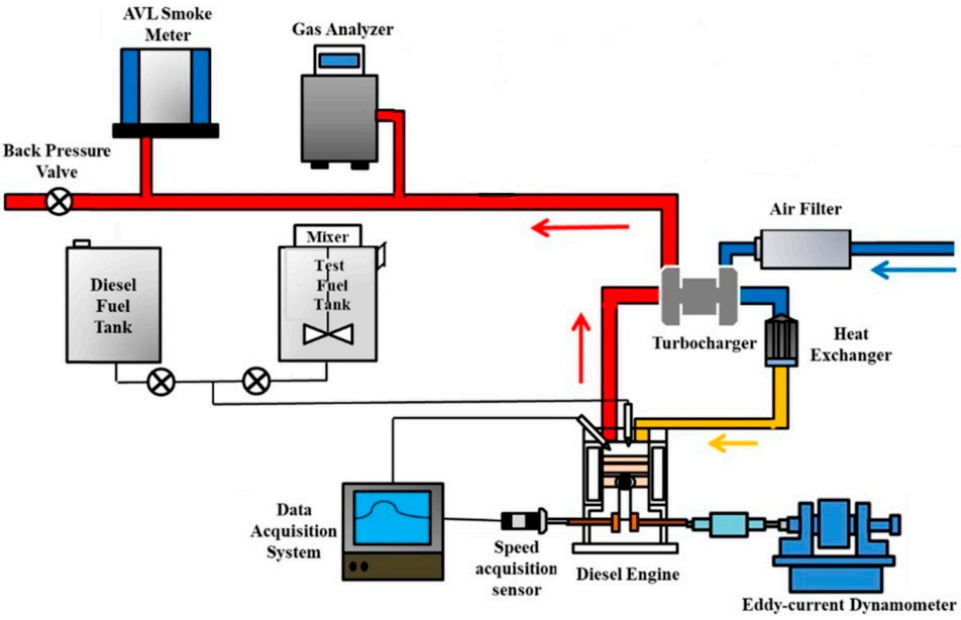


Figure 1. Schematic layout diagram of the experimental system.

Table 1. Engine specifications.

Item	Value
Engine type	Four-stroke compression ignition
Bore (mm)	86
Stoke (mm)	94.7
Displacement (L)	1.99
Number of valves	16
Compression ratio	16.5
Number of cylinders	4
Connecting rod (mm)	145.3
Maximum toque (N m)	290
Piston bowl design	w-bowl

Table 2. Engine operating conditions.

Item	Parameters
Speed (rpm)	1500
BMEP (MPa)	0.8
Injection pressure (MPa)	60, 80, 100, 120, 140, 160
Injections	Single
Injection time (°CA ATDC)	−4
Intake temperature (°C)	28 ± 3 °C
Intake pressure (bar)	1.5 ± 0.5
Coolant temperature (°C)	82 ± 2 °C

The heat release rate is a function of the variable ICP and is deduced according to the first law of thermodynamics. Hence, the heat release rate and combustion durations were inferred using a pressure trace. According to Heywood, the calculation formula for the heat release rate can be expressed as follows [33]:

$$\frac{dQ}{d\theta} = \frac{\gamma}{\gamma - 1} P \frac{dV}{d\theta} + \frac{1}{\gamma - 1} V \frac{dp}{d\theta} \quad (1)$$

where γ is the ratio of the specific heat (taken as 1.37 in this study), p is the ICP, and V is the instantaneous cylinder volume.

The concentrations of the exhaust emissions, including CO, HC, and NO_X, were measured using a Horiba MEXA 7100 DEGR. The soot was measured using an AVL-415SE filter-type smoke meter. In addition, the number of particles and their size distributions were measured with a particulate analyzer (TSI EEPS 3090, USA).

2.2. Test Fuels

To distinguish the oxygen concentration from the combustion and emissions in CI engines, the oxygen content of *n*-octanol/diesel blends was controlled to 0% (N0, pure diesel), 2.5% (N2.5, 20% *n*-octanol (*v*/*v*) and 80% diesel), and 5% (N5, 40% *n*-octanol (*v*/*v*), and 60% diesel), respectively. There was no need to add cetane improvers or surfactants owing to the properties of these fuels, such as their less-hygroscopic nature and relatively high CN numbers in comparison with other alcohols. The solubility of all mixtures was confirmed after several days of observation, and no phase separation was found. The properties of the blended fuels are listed in Table 3.

Table 3. Properties of blending fuels samples.

Properties	*n*-Octanol [a]	N0 [b]	N2.5	N5
Oxygen (wt%)	12.3	0	2.5	5
Cetane number	39	54	50.95	47.90
Density (kg/m^3)	830	837	835.57	834.15
Low heating value (MJ/kg)	37.53	42.80	41.73	40.66
Latent heat of evaporation (kJ/kg)	408	270	298.05	326.09
Kinematic viscosity (mm^2/s@40 °C)	5.50	3.04	3.54	4.04
Flash point (°C)	81	55	60.28	65.57

[a] Source: Ref [15], [b] Source: ASTM D975.

2.3. Total Uncertainty Analysis

In the process of the experiment, systematic and accidental errors were inevitable. Based on the error propagation principle, the total uncertainty equation is as follows [34]:

$$\sqrt{\sum U_i^2} = 0.364\% \quad (2)$$

where U_i is the uncertainty of i, with i representing speed, BMEP, pressure, time, CO, NO_X, and HC in turn. Table 4 shows the parameters of the above formula.

Table 4. Uncertainty analysis of the measured parameters.

Measurement Quantity	Percentage Uncertainty (%)
Speed (rpm)	±0.1
BMEP (MPa)	±0.2
Pressure (MPa)	±0.05
Time (s)	±0.2
CO/NO_X/HC (ppm)	±0.2

3. Result and Discussions

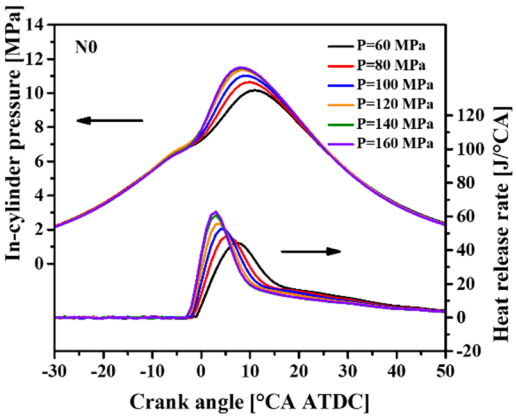
3.1. Combustion Characteristics

The combustion characteristics, such as the ICP and heat release rate (HRR), are the most crucial parameters directly affecting combustion characteristics, engine-out emissions, and power outputs [27]. Figure 2 shows that the ICP and HRR curves for the test fuels vary with the IP. The curves depict the nature of the maximum ICP rise along with the increased IP, and hence reflect the combustion quality. When the IP increases from 60 to 160 MPa, the peak values of the ICP for N0, N2.5, and N5 increase by approximately 13.11%, 13.14%, and 15.34%, respectively. This is because the injected fuel quantity per unit chamber increases with the increase in IP, thus increasing the ICP. A higher IP is beneficial to the secondary breakup of droplets, leading to a superior self-ignition effect [30]. As can be seen in Figure 3a, at a giving IP, with an increasing proportion of *n*-octanol, a slight drop in the peak ICP was shown. This is a result of the lower energy content of the *n*-octanol/diesel blend fuel. The position of the maximum ICP indicates the rate of this energy release, and it is mainly dependent on the oxygen structure, viscosity, and latent heat of evaporation (LHOE) of the fuel [35]. This also proves the relatively small impacts of the blending fuels on the ICP. Kumar et al. [36] researched the influence of IP on the performance of a biodiesel engine with a cerium oxide nanoparticle additive and obtained a similar result.

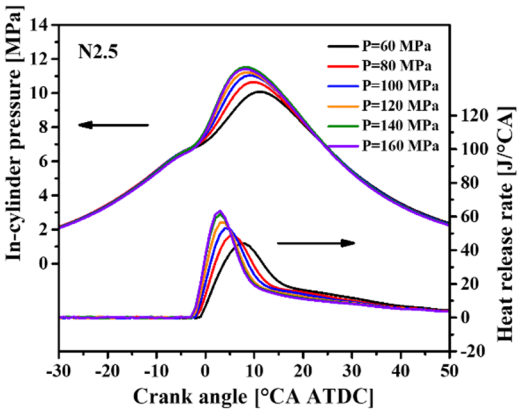
The HRR is a function of the variable ICP, and consequently follows the same change rules as the ICP, e.g., its peak value is increased with the increase in the IP. As the IP increases from 60 to 160 MPa, the maximum HRR values for N0, N2.5, and N5 increase by approximately 41.96%, 44.01%, and 43.42%, respectively. As mentioned above, the additional accumulated injected fuel quantity gives rise to rapid combustion, contributing to the higher HRR. In addition, a higher IP promotes the atomization and fuel–air mixture processes, contributing to a more complete combustion. As can be seen in Figure 3b, at a giving IP, the largest to smallest HRR peaks were arranged as N2.5 > N0 > N5, but the HRR peak gap among all test fuels was small. On the one hand, the laminar combustion rate of octanol isomers is also higher than that of diesel, promoting combustion [37]. On the other hand, *n*-octanol/diesel fuels have a lower energy content and higher viscosity relative to diesel, potentially leading to a lower HRR. Therefore, the peak HRR is the result from the internal competition of *n*-octanol. However, the introduction of *n*-octanol has little effect on the peaks of ICP and HRR.

The ID is a dynamic parameter representing the time interval between the beginning of fuel injection and combustion initiation. The variation in the ID with IP for the test fuels is depicted in Figure 4. The results show that, with increasing IP, the IDs of test fuels decreased. The trends were in line with the studies [38–40]. when the IP is less

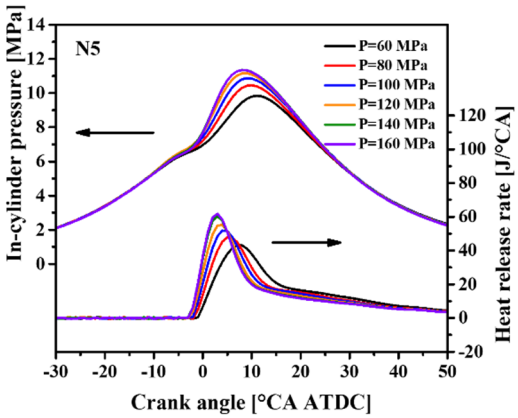
than 120 MPa, the ID presents an almost invisible increase with increases in the *n*-octanol proportion for the same pressure. Then, there is a slight delay when the IP is greater than 120 MPa. The results are in line with those of Prasad et al. [32], who concluded that the addition of butanol to pure diesel could prolong the ID. This phenomenon is attributed to the fuel properties, namely, the lower CN of *n*-octanol relative to diesel; its higher oxygen content and latent heat of vaporization also prolong the ID. In addition, the high viscosity worsens the evaporation and fuel atomization, as well as the mixing with air. The figure also shows that, for all of the test fuels, the ID varies inversely with the IP. When IP were 60–120 MPa, there were little differences in the ID values of test fuels. When the IP were increased to 140 and 160 MPa, The IDs of test fuels became obvious. The reason was that the injected fuel shows a smaller Sauter average diameter, shorter broken chain length, and greater dispersion and atomization, resulting in a shorter ID [41,42].



(**a**) The in-cylinder pressure and heat release rate of N0 at different injection pressures.



(**b**) The in-cylinder pressure and heat release rate of N2.5 at different injection pressures.

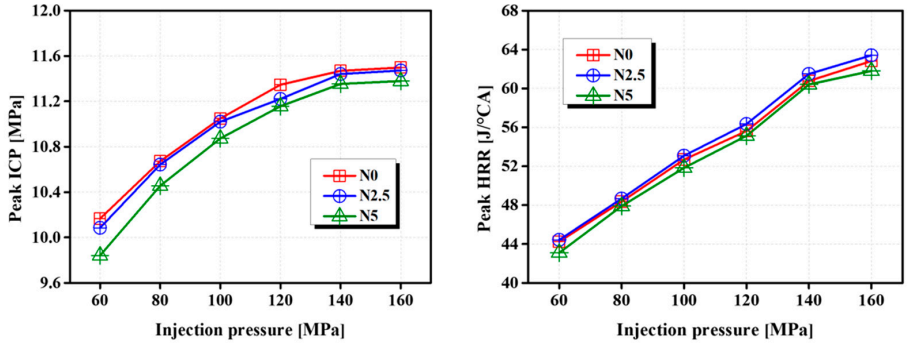


(**c**) The in-cylinder pressure and heat release rate of N5 at different injection pressures.

Figure 2. Variation of in-cylinder pressure and heat release rate with respect to injection pressure for *n*-octanol/diesel blends.

One of the key indicators for judging the combustion process and heat release performance is the combustion phase CA50, referring to the degree at which a 50% fuel mass fraction has been burned. Figure 5 presents the variation in the CA50 with IP for the *n*-octanol/diesel blends. As shown, at a giving IP, the longest to shortest CA50s were arranged as follows: N5 > N0 > N2.5. There were two reasons for this phenomenon. On the one hand, compared with pure diesel, *n*-octanol has higher oxygen concentrations and higher laminar burning velocities, which had a positive effect on shortening CA50 [43]. On the other hand, the LHOE and viscosity of *n*-octanol were higher than those of pure diesel, the atomization and fuel–air mixture processes became worse, and the

charge-cooling effect became stronger, which had a negative effect on shortening CA50 [40]. Consequently, an extension of CA50 of N5 is shown. Therefore, the CA50 is the result from the internal competition of the two aspects. Among all the test fuels, the CA50 of N5 was the largest, followed by N0, and N2.5 was the smallest. It is evident that, following the increase in IP, the trend of CA50 is a decline for all of the test fuels. This correlation is probably related to the HRR curves moving forward as the IP increases, as the HRR rises and shifts to an earlier corresponding phase. In addition, the atomization process is improved with successive increases in the intensity of IP as well as accelerated fuel–air mixing; therefore, the crank of CA50 advances remarkably.



(**a**) The peak ICP of test fuels at different injection pressures

(**b**) The peak HRR of test fuels at different injection pressures.

Figure 3. Variation of peaks ICP and HRR with respect to injection pressure for *n*-octanol/diesel blends.

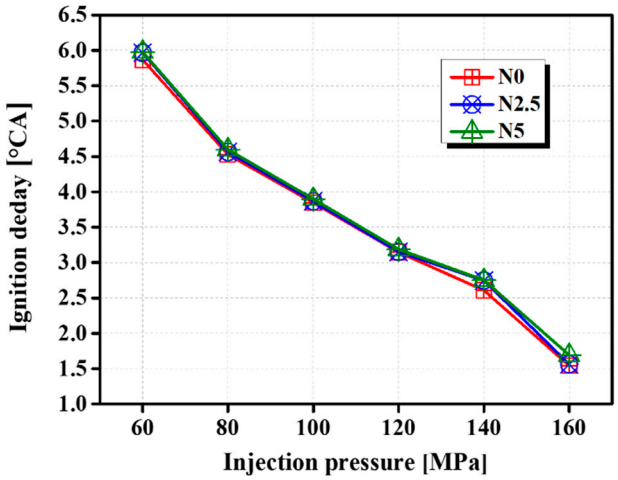


Figure 4. Variation in ignition delay with injection pressure for *n*-octanol/diesel blends.

Figure 6 reveals the variation in the maximum in-cylinder temperature (MICT) with IP for the test fuels. The results the correlational analysis show that, for the same level of fuel, with successive increases in the intensity of the IP, the MICT increases significantly. When the IP is boosted from 60 to 160 MPa, the response increase rates of the MICT are approximately 20.41%, 20.96%, and 19.13% for N0, N2.5, and N5, respectively. This is because a higher IP will arise with the faster rate of combustion, and as a result of that, a higher temperature is shown. Moreover, a higher IP leads to an increased HRR, owing to the better air-fuel mixture and premixed combustion. Furthermore, following the addition of *n*-octanol, the following order was found: N0 > N5 > N2.5. The major reason is that the higher LHOEs and lower heating values of the blends decrease the MICT in the cylinder as compared with diesel. Thus, the MICT values of the *n*-octanol/diesel blends are lower than

those for diesel. However, the higher oxygen content improves the combustion behavior and offers the possibility of complete combustion, leading to an increased MICT. Evidently, in this study, the oxygen content weakens the influence of the LHOE and lower heat value, and it shows a higher temperature for N5 than for N2.5.

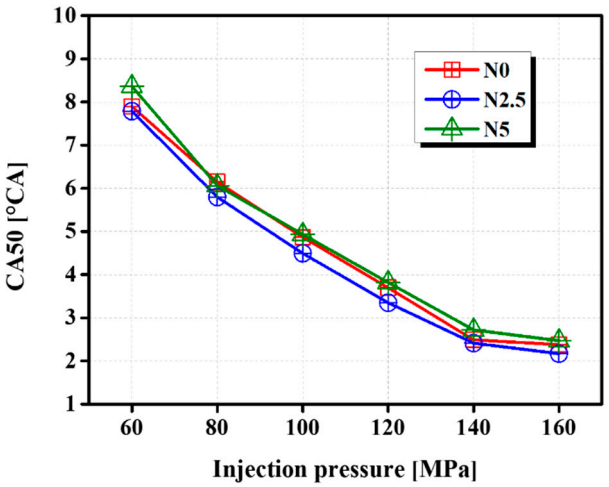


Figure 5. Variation in CA50 with injection pressure for *n*-octanol/diesel blends.

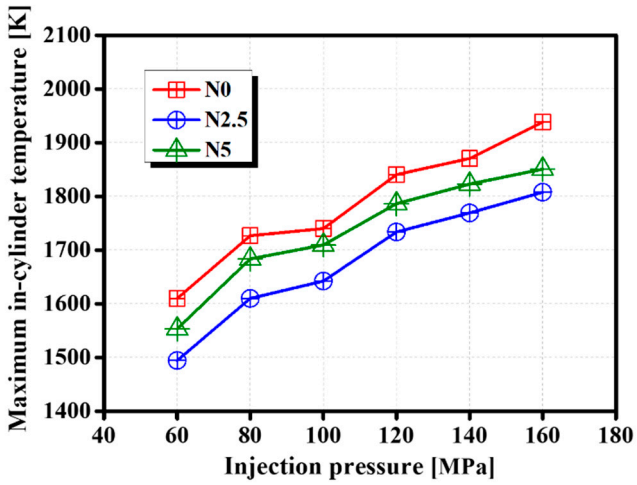


Figure 6. Variation in maximum in-cylinder temperature with injection pressure for *n*-octanol/diesel blends.

The BSFC is defined as the ratio of fuel consumption to brake power, and it is an important economic index. Figure 7 shows the change in the BSFC according to the IP for the test fuels. The BSFC slowly decreased with the increase in IP. This decline in the BSFC is the result of the larger jet penetration of the fuel spray and smaller droplet size contributing to the air–fuel mixture; as a result, the ID and BSFC are reduced. There is a slight upward trend after 120 MPa. This is because the ID will be too short if the IP is too high. In such cases, the homogeneous mixed period decreases, leading to a relatively bad combustion efficiency and lower power output [27,29], and in generating the specified brake power for the engine, lead to additional fuel consumption. Moreover, at the same level of IP, the BSFC increases with an increasing blending ratio of *n*-octanol, owing to the decrease in the energy content [37]. N5, which has the lowest heat value, has the highest BSFC per IP. *n*-Octanol has a higher LHOE in comparison with pure diesel and draws more heat from the process of fuel vaporization. Hence, the lower fuel conversion efficiency

results in a higher BSFC [35]. In addition, the higher viscosity of the *n*-octanol worsens the fuel atomization, leading to an increase in the BSFC.

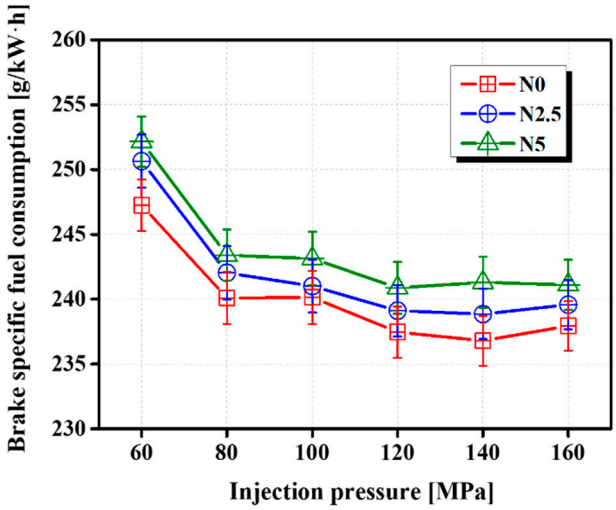


Figure 7. Curve analysis of brake specific fuel consumption according to injection pressure for *n*-octanol/diesel blends.

The BTE assesses the efficiency of energy conversion from fuels into mechanical outputs [31]. Figure 8 presents the change in BTE according to the IP for the *n*-octanol/diesel blend fuels. The BTE is a function of the low heating values and BSFCs of the blends at a constant effective power. The highest BTE was 36.3%, for N5 at 120 MPa. As noted above, a higher IP is beneficial to combustion. If the IP is too high, the homogeneous mixed period decreases, resulting in poor combustion efficiency; therefore, the BTE decreases. It was also found that, when the IP is constant, the BTE increases by an average of 1.4% with an increase in oxygen content. One possible reason is that the higher oxygen content enables complete combustion, achieving a higher combustion efficiency, and hence improving the BTE. Another reason is that *n*-octanol has a lower molecular weight than diesel; this implies that less energy is consumed in the process of fuel degradation, consequently improving the fuel conversion efficiency [35]. The results in this section indicate that the best BTE and BSFC values are obtained at 120 MPa.

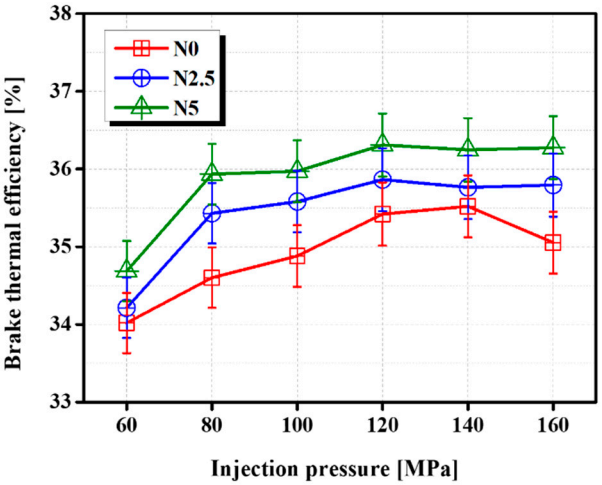


Figure 8. Curve analysis of brake thermal efficiency according to injection pressure for *n*-octanol/diesel blends.

3.2. Exhaust Emissions

The factors that mainly affect CO emission formation are the air–fuel ratio, fuel type, fuel atomization rate, IP, and timing [41]. CO is oxidized to CO_2 when the oxygen concentration is sufficient in the cylinder. Therefore, the air–fuel equivalence ratio is the primary factor controlling the formation of CO. The CO emissions at different IPs for the *n*-octanol/diesel blends are presented in Figure 9. CO emissions were found to decrease with the addition of *n*-octanol. One possible reason is that the use of *n*-octanol increases the number of active radicals of OH, O, and H, promoting CO oxidation by the reaction path as CO + OH = CO_2 + H and O + CO + M = CO_2 + M [32], in addition to the lower C/H ratio of *n*-octanol relative to diesel. We also observed that, when the test fuel remains unchanged, as the intensity of IP increases, the CO decreases first, and then increases. The CO emissions of N5 at 100 MPa drop by approximately 32% when compared with the operating condition of 60 MPa. This is because increasing both the IP and viscosity of *n*-octanol causes a quicker and earlier injection timing, enhancing the mixture of air and fuel in the combustion chamber, and thereby decreasing CO emissions [31]. However, the higher is the IP, the shorter is the combustion duration, and there may not be sufficient time for complete oxidization. Therefore, the IP has positive and negative effects on CO, and considering the various aspects comprehensively is necessary to achieve better CO emissions in the design of diesel engines.

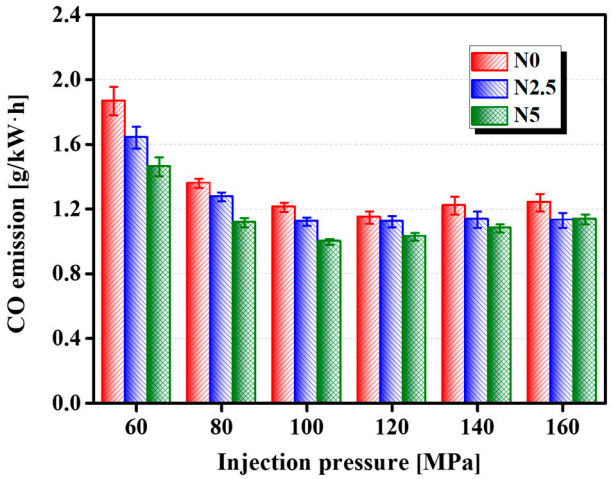


Figure 9. CO emissions of different injection pressures for *n*-octanol/diesel blend fuels.

The process of forming HCs is largely related to the lack of oxygen required for complete combustion [44]. Figure 10 presents the HC emissions of different IPs for the *n*-octanol/diesel blends. As the dosage of *n*-octanol additives increases, the HC emissions increase slightly. This may be owing to the unnecessary fuel impingement on the combustion chamber wall [11]. The higher enthalpy of evaporation relative to diesel results in a lower flame temperature and combustion quenching. Additionally, the relatively higher viscosity is harmful to atomization; hence, the burning of the fuel fraction is less in the premixed stage, and more in the mixing-control stage. As a result, it is difficult to achieve complete oxidation of the burned HCs before the exhaust valve is opened [35]. However, the HC emissions decrease evidently with the increase in IP. This is because a higher IP achieves more atomization and improves the fuel–air mixture, benefitting engine combustion and reducing HC emissions. In this study, the amount of HC emissions is the result of competition between the nature of the *n*-octanol and IP. We can observe that a high IP (>100 MPa) decreases the adverse impact of *n*-octanol and shows lower HC emissions than that of N0. The best effect is obtained at 160 MPa for N2.5.

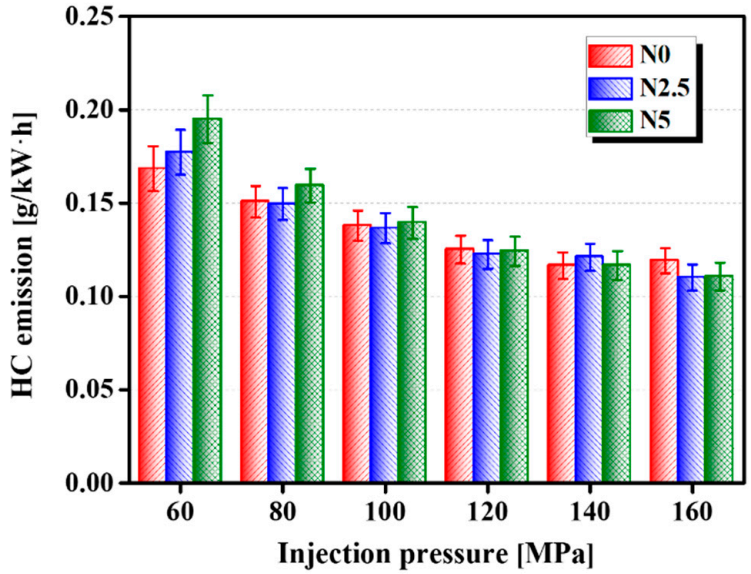


Figure 10. HC emissions of different injection pressures for *n*-octanol/diesel blends.

The formation of NO_X is mainly based on the Zeldovich mechanism, i.e., a thermal NO_X mechanism related to the peak temperature of the combustion gas, oxygen content, and gas residence time of the reaction [45]. Figure 11 shows the NO_X emissions at different IPs for the *n*-octanol/diesel blends. As shown, the introduction of *n*-octanol into diesel, results in a decline of NO_X; notwithstanding this, the NO_X amounts at all test IPs from highest to lowest are: N0 > N5 > N2.5. One possible reason is that, compared with diesel, *n*-octanol (with a higher LHOE) decreases the in-cylinder combustion temperature, thereby decreasing NO_X emissions [41]. Thus, *n*-octanol/diesel blends have lower levels of NO_X emissions than diesel. However, their higher oxygen content accelerates the combustion, giving rise to higher local temperatures owing to excessive HC oxidation this is in accordance with the higher HCs in Figure 10. As a result, the NO_X emission of N5 is higher than that of N2.5. The figure shows that the NO_X increases with increasing IP but also that the uptrend gradually flattens, and even shows a slightly descending trend. This is because a higher IP decreases the particle diameter and offers higher kinetic energy, thereby generating a faster rate of combustion, which contributes to the higher temperature and consequently higher NO_X emission. However, a shorter ID decreases the NO_X chemistry reactions [36].

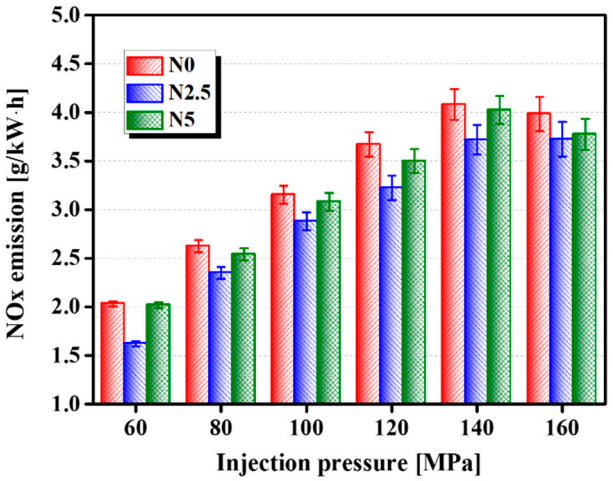


Figure 11. NO_X emissions of different injection pressures for *n*-octanol/diesel blends.

A large part of soot emission formation is dependent upon high temperatures and oxygen deficiencies [46]. For long-chain molecules, soot is produced by anoxic pyrolysis. The soot emissions at different IPs for the test fuels are shown in Figure 12. No matter what type of fuel, as the IP increases, the soot emissions first decrease, and then present a small increase. One possible reason is that boosting the IP promotes the formation of smaller fuel droplets, which is conducive to better dispersion and mixing; therefore, the soot is reduced. However, a higher IP results in a shorter ID, which weakens the premix period; moreover, oxygen deficiencies exist locally. In addition, the average percentages of declinable soot emissions for N2.5 and N5 are approximately 9% and 18%, respectively. One explanation could be that the oxygen content increases with an increase in the *n*-octanol proportion; this reduces fuel-rich zones and improves the oxidation of soot. Similarly, the OH group in *n*-octanol fuels intensifies combustion and accelerates soot oxidation in the flame zone [47]. Therefore, the soot emissions decrease with an increase in the *n*-octanol proportion.

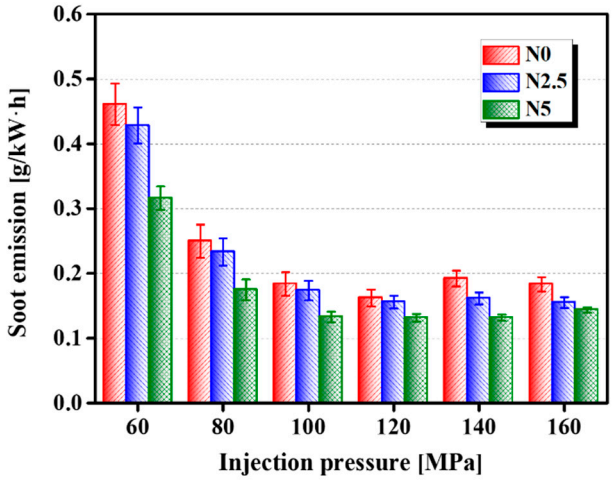
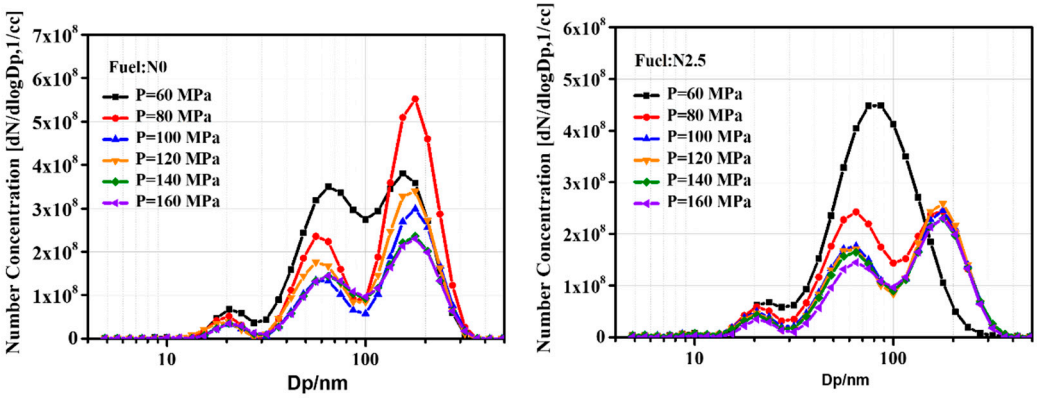


Figure 12. Soot emissions of different injection pressures for *n*-octanol/diesel blends.

In regards to particle size, particles can generally be classified as either a nucleation model particle (NMP) with a diameter less than 50 nm (the formation of these is related to the nucleation, condensation, and coagulation of the unburned HC) or an accumulation mode particle with a diameter between 50 and 1000 nm (these are usually formed by the adsorption of organic and inorganic compounds) [48,49]. In general, the primary soot concentration, dilution ratio, and temperature significantly affect the particle size distribution (PSD) [16]. In addition, the final distribution is dependent on both particle formation and oxidation [50].

Figure 13 depicts the PSD under different IPs for the test fuels. As shown in Figure 13a and b, the particle size is distributed trimodally. For the N5 (Figure 13c) condition, the size distribution changes, and the particle size generally shows bimodal distributions. It can be observed that the PSD curves move forward with additional proportions of *n*-octanol. The effect of the oxygenated fuels dramatically reduces the large particle number concentrations, as proven by Lapuerta et al. [51]. The higher is the proportion of *n*-octanol, the lower are the soot emissions and the lower is the primary soot concentration. In addition, oxygenated fuels together with higher temperatures cause a more active oxidation process [38]. Both the low primary soot concentration and high temperature factors favor a decline in particle size. However, the number of NMPs increases. As illustrated in Figure 10, the amount of HC increases slightly with an increase in *n*-octanol. Therefore, the amount of unburned HC increases marginally. It is also apparent from these figures that, with the increase in intensity of IP, the particle number decreases markedly, and no significant differences are found in the particle size. The reason may be that the higher IP causes relatively preferable fuel–air mixing, and hence a better combustion state [27]. In addition, a lower ID shortens the polymerization time, further lowering the particle number [52]. However, for the entire

distribution, the particle size is still mostly distributed within the accumulation modes, irrespective of the condition of fuel types and IPs.



(**a**) The particle matter size distributions of N0 under different injection pressures.

(**b**) The particle matter size distributions of N2.5 under different injection pressures.

(**c**) The particle matter size distributions of N5 under different injection pressures.

Figure 13. Particle matter size distributions under different injection pressures for *n*-octanol/diesel blends.

The relationship between soot and NO_X still hinders the development of CI engines, owing to the opposite formation condition. Figure 14 depicts the relationship curves between soot and NO_X emissions of *n*-octanol/diesel blends at different IPs. No matter the type of test fuel, with increased IP, the soot emissions present a change of "down then up slightly", whereas the NO_X emissions increase first, and then tends to be gentle. When the IP remains constant, along with the increased ratio of *n*-octanol blending, the soot emissions decline, and the NO_X emissions exhibit a regular change of: N0 > N5 > N2.5. Therefore, there exists a best point or range for realizing a balanced effect of both soot and NO_X. In this figure, it seems to be at 100 MPa, as fueled with N5.

The relationship between the BTE and CO is statistically significant for characterizing the combustion effect. Higher levels of CO emissions indicate an incomplete energy conversion, which is also reflected in a lower BTE. Figure 15 is a graph showing the effect of IP on the relationship between the BTE and CO of the test fuels. As shown, under the same IP, with an increase in the mixed proportion of *n*-octanol, the BTE increases while the CO decreases. Furthermore, along with the boost of the IP, the BTE and CO show a reverse change trend. The variation of the BTE increases first and then decreases fractionally, and the CO decreases first and then increases slightly. From this analysis, both the *n*-octanol content and IP favor complete combustion. Similarly, the most satisfactory level is achieved at 100 or 120 MPa, when burning with N5.

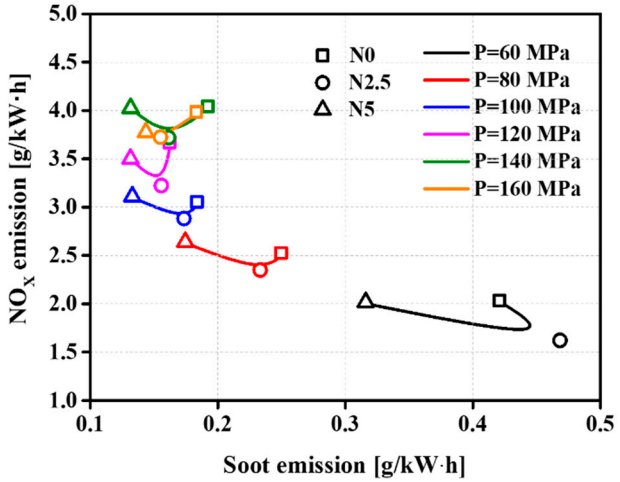


Figure 14. Soot–NOX relationship of *n*-octanol/diesel blends with different injection pressures.

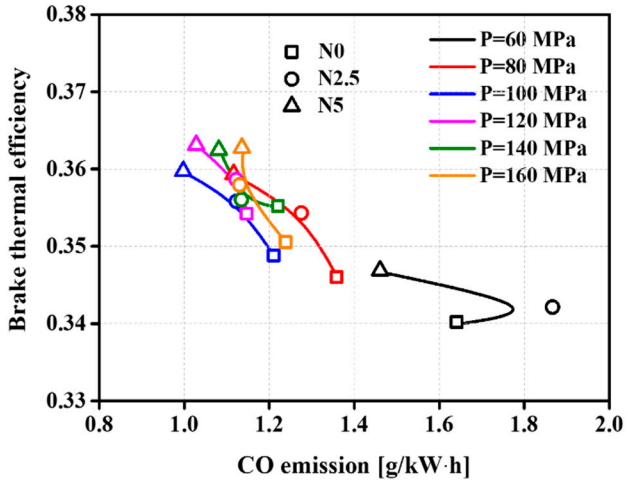


Figure 15. Brake thermal efficiency–CO relationship of *n*-octanol/diesel blends with different injection pressures.

4. Conclusions

To study the combustion and emission performances of burning oxygenated fuels in diesel engines, we investigated the effects of *n*-octanol/diesel blends (N0, N2.5, and N5) as combined with IPs (ranging from 80 to 160 MPa) on a turbocharged, four-cylinder diesel engine, and discussed the optimum results. According to the experimental results, the following conclusions can be drawn.

1. The blending fuels have little influence on the ICP, ID times, and CA50, but they improve the BTE.
2. The BTE increases and BSFC decreases with an increase in the IP. The best effect for both was obtained at 120 MPa.
3. After adding *n*-octanol to diesel, the exhaust emissions of CO and NO_X decrease, whereas the HC emissions increase slightly. With a boost of the IP, the CO and HC emissions decrease, whereas the NO_X increases.
4. Soot emissions decrease with increasing IP and *n*-octanol values. The size of the accumulation mode particle decreases significantly with increasing *n*-octanol, and achieves the lowest particle number at 100 MPa with N5.
5. The optimum effects of combustion and emission are obtained at 100 or 120 MPa with N5.

Author Contributions: Conceptualization, methodology, supervision, writing-original draft, Q.W.; data curation, investigation, writing-review & editing, R.H.; project administration, resources, J.N. formal analysis, Q.C. All authors have read and agreed to the published version of the manuscript.

Funding: This research received no external funding.

Institutional Review Board Statement: Not applicable.

Informed Consent Statement: Informed consent was obtained from all subjects involved in the study.

Data Availability Statement: No new data were created or analyzed in this study. Data sharing is not applicable to this article.

Acknowledgments: This work was supported by the Natural Science Foundation of Shanghai (grant number 16ZR1438500).

Conflicts of Interest: The authors declare no conflict of interest.

Abbreviations

BTE	brake thermal efficiency
BSFC	brake specific fuel consumption
BMEP	brake mean effective pressure
CI	compression ignition
CO	carbon monoxide
CN	cetane number
HRR	heat release rate
HC	hydrocarbon
IP	injection pressure
ID	ignition delay
ICP	in-cylinder pressure
LHOE	latent heat of evaporation
MICT	maximum in-cylinder temperature
N0	pure diesel
N2.5	2.5% oxygen content in blending fuels
N5	5% oxygen content in blending fuels
NO_X	nitrogen oxides
NMP	nucleation mode particles
PM	particulate matter
PSD	particle size distribution

References

1. Kalghatgi, G.T. The outlook for fuels for internal combustion engines. *Int. J. Engine Res.* **2014**, *15*, 383–398. [CrossRef]
2. Escobar, J.C.; Lora, E.S.; Venturini, O.J.; Yanez, E.E.; Castillo, E.F.; Almazan, O. Biofuels: Environment, technology and food security. *Renew. Sustain. Energy Rev.* **2009**, *13*, 1275–1287. [CrossRef]
3. Laden, F.; Schwartz, J.; Speizer, F.E.; Dockery, D.W. Reduction in fine particulate air pollution and mortality: Extended follow-up of the Harvard Six Cities study. *Am. J. Respir. Crit. Care Med.* **2006**, *173*, 667–672. [CrossRef]
4. Hu, E.; Chen, Y.; Zhang, Z.; Chen, J.-Y.; Huang, Z. Ab initio calculation and kinetic modeling study of diethyl ether ignition with application toward a skeletal mechanism for CI engine modeling. *Fuel* **2017**, *209*, 509–520. [CrossRef]
5. Gu, X.; Huang, Z.; Cai, J.; Gong, J.; Wu, X.; Lee, C.-F. Emission characteristics of a spark-ignition engine fuelled with gasoline-*n*-butanol blends in combination with EGR. *Fuel* **2012**, *93*, 611–617. [CrossRef]
6. Wang, X.; Huang, Z.; Kuti, O.A.; Zhang, W.; Nishida, K. An experimental investigation on spray, ignition and combustion characteristics of biodiesels. *Proc. Combust. Inst.* **2011**, *33*, 2071–2077. [CrossRef]
7. Hawi, M.; Kosaka, H.; Sato, S.; Nagasawa, T.; Elwardany, A.; Ahmed, M. Effect of injection pressure and ambient densityon spray characteristics of diesel and biodiesel surrogate fuels. *Fuel* **2019**, *254*, 115674. [CrossRef]
8. Wang, Q.; Yin, S.; Ni, J. The effects of n-pentanol, di-*n*-butyl ether (DBE) and exhaust gas recirculation on performance and emissions in a compression ignition engine. *Fuel* **2021**, *284*, 118961. [CrossRef]
9. Çelebi, Y.; Aydın, H. An overview on the light alcohol fuels in diesel engines. *Fuel* **2019**, *236*, 890–911. [CrossRef]
10. Emiroğlu, A.O. Effect of fuel injection pressure on the characteristics of single cylinder diesel engine powered by butanol-diesel blend. *Fuel* **2019**, *256*, 115928. [CrossRef]

11. Ardebili, S.M.S.; Solmaz, H.; Ipci, D.; Calam, A.; Mostafaei, M. A review on higher alcohol of fusel oil as a renewable fuel for internal combustion engines: Applications, challenges, and global potential. *Fuel* **2020**, *279*, 118516. [CrossRef]
12. Campos-Fernández, J.; Arnal, J.M.; Gómez, J.; Dorado, M.P. A comparison of performance of higher alcohols/diesel fuel blends in a diesel engine. *Appl. Energy* **2012**, *95*, 267–275. [CrossRef]
13. Akhtar, M.K.; Dandapani, H.; Thiel, K.; Jones, P.R. Microbial production of 1-octanol: A naturally excreted biofuel with diesel-like properties. *Metab. Eng. Commun.* **2015**, *2*, 1–5. [CrossRef] [PubMed]
14. Doğan, O. The influence of n-butanol/diesel fuel blends utilization on a small diesel engine performance and emissions. *Fuel* **2011**, *90*, 2467–2472. [CrossRef]
15. Kumar, B.R.; Saravanan, S. Use of higher alcohol biofuels in diesel engines: A review. *Renew. Sustain. Energy Rev.* **2016**, *60*, 84–115. [CrossRef]
16. Preuß, J.; Munch, K.; Denbratt, I. Performance and emissions of long-chain alcohols as drop-in fuels for heavy duty compression ignition engines. *Fuel* **2018**, *216*, 890–897. [CrossRef]
17. Jin, C.; Yao, M.; Liu, H.; Lee, C.-F.F.; Ji, J. Progress in the production and application of n-butanol as a biofuel. *Renew. Sustain. Energy Rev.* **2011**, *15*, 4080–4106. [CrossRef]
18. Heuser, B.; Kremer, F.; Pischinger, S.; Julis, J.; Leitner, W. *Optimization of Diesel Combustion and Emissions with Newly Derived Biogenic Alcohols*; SAE Technical Paper Series; SAE International: Troy, MI, USA, 2013.
19. Hoppe, F.; Heuser, B.; Thewes, M.; Kremer, F.; Pischinger, S.; Dahmen, M.; Hechinger, M.; Marquardt, W. Tailor-made fuels for future engine concepts. *Int. J. Engine Res.* **2015**, *17*, 16–27. [CrossRef]
20. Deep, A.; Kumar, N.; Karnwal, A.; Gupta, D.; Vibhanshu, V.; Sharma, A.; Patel, J.S. *Assessment of the Performance and Emission Characteristics of 1-Octanol/Diesel Fuel Blends in a Water Cooled Compression Ignition Engine*; SAE Technical Paper Series; SAE International: Troy, MI, USA, 2014.
21. McCormick, R.L.; Ross, J.D.; Graboski, M.S. Effect of several oxygenates on regulated emissions from heavy-duty diesel engines. *Environ. Sci. Technol.* **1997**, *31*, 1144–1150. [CrossRef]
22. Phoon, L.Y.; Mustaffa, A.A.; Hashim, H.; Mat, R.; Manan, Z.A.; Yunus, N.A. Performance and emission characteristics of green diesel blends containing dieth-yl-succinate and 1-octanol. *J. Clean. Prod.* **2017**, *161*, 1192–1202. [CrossRef]
23. Zhang, T.; Munch, K.; Denbratt, I. An Experimental Study on the Use of Butanol or Octanol Blends in a Heavy Duty Diesel Engine. *SAE Int. J. Fuels Lubr.* **2015**, *8*, 610–621. [CrossRef]
24. Cai, L.; Uygun, Y.; Togbé, C.; Pitsch, H.; Olivier, H.; Dagaut, P.; Sarathy, S.M. An experimental and modeling study of *n*-octanol combustion. *Proc. Combust. Inst.* **2015**, *35*, 419–427. [CrossRef]
25. Bharti, A.; Banerjee, T. Reactive force field simulation studies on the combustion behavior of *n*-octanol. *Fuel Process. Technol.* **2016**, *152*, 132–139. [CrossRef]
26. Kerschgens, B.; Cai, L.; Pitsch, H.G.; Heuser, B.; Pischinger, S. Di-*n*-buthylether, *n*-octanol, and *n*-octane as fuel candidates for diesel engine combustion. *Combust. Flame* **2016**, *163*, 66–78. [CrossRef]
27. Agarwal, A.K.; Srivastava, D.K.; Dhar, A.; Maurya, M.K.; Shukla, P.C.; Singh, A.P. Effect of fuel injection timing and pressure on combustion, emissions and performance characteristics of a single cylinder diesel engine. *Fuel* **2013**, *111*, 374–383. [CrossRef]
28. Zhang, G.; Qiao, X.; Miao, X.; Hong, J.; Zheng, J. Effects of highly dispersed spray nozzle on fuel injection characteristics and emissions of heavy-duty diesel engine. *Fuel* **2012**, *102*, 666–673. [CrossRef]
29. Çelıkten, I. An experimental investigation of the effect of the injection pressure on engine performance and exhaust emission in indirect injection diesel engines. *Appl. Therm. Eng.* **2003**, *23*, 2051–2060. [CrossRef]
30. Kuszewski, H. Effect of Injection Pressure and Air–Fuel Ratio on the Self-Ignition Properties of 1-Butanol–Diesel Fuel Blends: Study Using a Constant-Volume Combustion Chamber. *Energy Fuels* **2019**, *33*, 2335–2347. [CrossRef]
31. Gumus, M.; Sayin, C.; Canakci, M. The impact of fuel injection pressure on the exhaust emissions of a direct injection diesel engine fueled with biodiesel–diesel fuel blends. *Fuel* **2012**, *95*, 486–494. [CrossRef]
32. Puhan, S.; Jegan, R.; Balasubbramanian, K.; Nagarajan, G. Effect of injection pressure on performance, emission and combustion characteristics of high linolenic linseed oil methyl ester in a DI diesel engine. *Renew. Energy* **2009**, *34*, 1227–1233. [CrossRef]
33. Heywood, J.B. *Internal Combustion Engine Fundamentals*; McGraw Hill: New York, NY, USA, 1988.
34. Holman, J.P. *Experimental Methods for Engineers*; McGraw Hill: New York, NY, USA, 2012.
35. Nour, M.; Attia, A.M.A.; Nada, S.A. Combustion, performance and emission analysis of diesel engine fuelled by higher alcohols (butanol, octanol and heptanol)/diesel blends. *Energy Convers. Manag.* **2019**, *185*, 313–329. [CrossRef]
36. Kumar, S.; Dinesha, P.; Rosen, M.A. Effect of injection pressure on the combustion, performance and emission characteristics of a biodiesel engine with cerium oxide nanoparticle additive. *Energy* **2019**, *185*, 1163–1173. [CrossRef]
37. Rajasekaran, S.; Damodharan, D.; Gopal, K.; Kumar, B.R.; De Poures, M.V. Collective influence of 1-decanol addition, injection pressure and EGR on diesel engine characteristics fueled with diesel/LDPE oil blends. *Fuel* **2020**, *277*, 118166. [CrossRef]
38. Huang, H.; Teng, W.; Li, Z.; Liu, Q.; Wang, Q.; Pan, M. Improvement of emission characteristics and maximum pressure rise rate of diesel engines fueled with n-butanol/PODE3-4/diesel blends at high injection pressure. *Energy Convers. Manag.* **2017**, *152*, 45–56. [CrossRef]
39. Khandal, S.V.; Banapurmath, N.R.; Gaitonde, V.N. Effect of exhaust gas recirculation, fuel injection pressure and injection timing on the performance of common rail direct injection engine powered with honge biodiesel (BHO). *Energy* **2017**, *139*, 828–841. [CrossRef]

40. Wu, H.; Nithyanandan, K.; Zhang, J.; Lin, Y.; Lee, T.H.; Lee, C.-F.F.; Zhang, C. Impacts of Acetone–Butanol–Ethanol (ABE) ratio on spray and combustion characteristics of ABE–diesel blends. *Appl. Energy* **2015**, *149*, 367–378. [CrossRef]
41. Ozsezen, A.N.; Canakci, M.; Sayin, C. Effects of biodiesel from used frying palm oil on the exhaust emissions of an indirect injection (IDI) diesel engine. *Energy Fuels* **2008**, *22*, 2796–2804. [CrossRef]
42. Prasad, K.S.; Rao, S.S.; Raju, V.R.K. Effect of compression ratio and fuel injection pressure on the characteristics of a CI engine operating with butanol/diesel blends. *Alex. Eng. J.* **2020**, *60*, 1183–1197. [CrossRef]
43. Zhang, T.; Nilsson, L.J.; Björkholtz, C.; Munch, K.; Denbratt, I. Effect of using butanol and octanol isomers on engine performance of steady state and cold start ability in different types of Diesel engines. *Fuel* **2016**, *184*, 708–717. [CrossRef]
44. Canakci, M.; Sayin, C.; Ozsezen, A.N.; Turkcan, A. Effect of Injection Pressure on the Combustion, Performance, and Emission Characteristics of a Diesel Engine Fueled with Methanol-blended Diesel Fuel. *Energy Fuels* **2009**, *23*, 2908–2920. [CrossRef]
45. Atmanli, A.; Yilmaz, N. A comparative analysis of n-butanol/diesel and 1-pentanol/diesel blends in a compression ignition engine. *Fuel* **2018**, *234*, 161–169. [CrossRef]
46. Wei, J.; Fan, C.; Qiu, L.; Qian, Y.; Wang, C.; Teng, Q.; Pan, M. Impact of methanol alternative fuel on oxidation reactivity of soot emissions from a modern CI engine. *Fuel* **2020**, *268*, 117352. [CrossRef]
47. Shi, C.; Ji, C.; Wang, S.; Yang, J.; Ma, Z.; Meng, H. Potential improvement in combustion behavior of a downsized rotary engine by intake oxygen enrichment. *Energy Convers. Manag.* **2020**, *205*, 112433. [CrossRef]
48. Li, Z.; Liu, G.; Cui, X.; Sun, X.; Li, S.; Qian, Y.; Jiang, C.; Lu, X. Effects of the variation in diesel fuel components on the particulate matter and unregulated gaseous emissions from a common rail diesel engine. *Fuel* **2018**, *232*, 279–289. [CrossRef]
49. Macián, V.; Bermúdez, V.; Villalta, D.; Soto, L. Effects of low-pressure EGR on gaseous emissions and particle size distribution from a dual-mode dual-fuel (DMDF) concept in a medium-duty engine. *Appl. Therm. Eng.* **2019**, *163*, 114245. [CrossRef]
50. Su, W.; Liu, B.; Wang, H.; Huang, H. Effects of Multi-Injection Mode on Diesel Homogeneous Charge Compression Ignition Combustion. *J. Eng. Gas Turbines Power* **2006**, *129*, 230–238. [CrossRef]
51. Lapuerta, M.; Armas, O.; Rodríguez-Fernández, J. Effect of biodiesel fuels on diesel engine emissions. *Prog. Energy Combust. Sci.* **2008**, *34*, 198–223. [CrossRef]
52. Seong, H.J.; Boehman, A.L. Studies of soot oxidative reactivity using a diffusion flame burner. *Combust. Flame* **2012**, *159*, 1864–1875. [CrossRef]